Neural, Parallel, and Scientific Computations 23 (2015) 87-110

COMPLEX DYNAMICS OF A FORCED DISCRETE VIRAL INFECTION MODEL WITH VIRUS-DRIVEN PROLIFERATION OF TARGET CELLS

A. ELHASSANEIN

Dept. of Math., Faculty of Science, Damanhour University, Damanhour, Egypt

ABSTRACT. In this paper, a forced discrete chaotic viral infection model with virus-driven proliferation of target cells is presented. The chaotic behavior of the proposed model is investigated. The existence and stability of the equilibria of the skeleton are studied. Numerical simulations are employed to show the model's complex dynamics by means of the largest Lyapunov exponents, bifurcations, time series diagrams and phase portraits. Time series diagrams are used to follow the dynamics of the model and discuss the marginal distribution of the state variables. The effects of noise intensity on its dynamics and the intermittency phenomenon are also discussed via simulation. An indicator of the chaotic behaviour of the asymptotic distribution of the stochastic systems is given.

AMS (MOS) Subject Classification. 37N25; 37G35; 37M10; 37F10; 37H10.

Keywords. Stochastic systems; In-host models; Skeleton; Bifurcations;Time series portraits; Phase diagrams; Chaos.

1. INTRODUCTION

The analysis of nonlinear dynamical systems (deterministic and stochastic) has received much attention from researchers in various fields, including physics, biology, mathematics, engineering, etc., see [5, 8, 12–14, 18–20, 25, 27, 35]. In recent years there has been an increasing interest in *in vivo* dynamics of viral infections. Most existing mathematical models for viral infection are described by systems of ordinary differential equations (ODEs), see [29, 32, 34, 36, 37]. Nowak and May [32] introduced the standard in-host model, which describes the interactions among healthy target cells $x(t)$, infected virus-producing cells $y(t)$ and free virus particles $\upsilon(t)$ in the following form:

$$\begin{cases} \dot{x} &= \lambda - dx(t) - \beta x(t)\upsilon(t) \\ \dot{y} &= \beta x(t)\upsilon(t) - ay(t) \\ \dot{\upsilon} &= ky(t) - u\upsilon(t), \end{cases}$$

where, λ is the production rate of uninfected target cells, which die at rate $dx(t)$, $\beta x(t)\upsilon(t)$ is the rate of infection of target cells by free virus, which die at rate $ay(t)$,

Received March 15, 2015

and $ky(t)$ is the rate of the production of new virus from infected cells, which die at rate $uv(t)$.The average life-time of uninfected cells, infected cells, and free virus is thus given by $1/d, 1/a$, and $1/u$, respectively. The average number of virus particles produced over the lifetime of a single infected cell (the burst size) is given by k/a, see also [1, 3, 6, 7, 9, 11, 24]. The proliferation of healthy T cells in the presence of virus is often neglected in many in-host models. However, it is known that both $CD8^+$ and $CD4^+T$ cells specific to HIV can be directly stimulated, and that activated T cells can stimulate other $CD8^+$ and $CD4^+$, [26]. Taking this into account, Shu and Wang [34] introduced a general viral model with virus-driven proliferation of target cells in the following form:

$$\left\{\begin{array}{lcl} \dot{T} &=& f(T,V) - k_1 h(T) g(V) \\ \dot{T^i} &=& k_1 h(T) g(V) - \mu_2 p(T^i) \\ \dot{V} &=& N\mu_2 p(T^i) - \mu_3 q(V) - k_2 h(T) g(V), \end{array}\right. \tag{1.1}$$

where the function $f(T,V)$ denotes the intrinsic growth rate of the healthy T cells, which includes the source of new T cells from the thymus, the natural mortality of cells and the stimulation of T cells to proliferate in the presence of virus, $k_1 h(T)g(V)$ is the rate of new infections of T cells, which includes the rate of contact between free virions and healthy T cells as well as the probability of cell entry per contact, $\mu_2 p(T^i)$ is the rate of death of the infected cells, N id the number new virions, $\mu_3 q(V)$ is the natural death rate of free virions, $k_2 h(T)g(V)$ is the loss of free infectious virions when they enter target cells, and k_2 is assumed to satisfy $k_2 < Nk_1$. Recently there has been an increasing interest in stochastic systems, see [10, 15, 16, 21, 22, 28, 30, 31, 38]. Parameters estimation of stochastic models is the most essential and critical problem in parametric analysis.

The main objectives of this paper are: to present a new stochastic discrete viral infection model with virus-driven proliferation of target cells; to investigate parameters changes effects on the dynamics of the proposed model; to give a numerical evidence about the chaotic behaviour of stochastic systems; and to give a novel chaotic 3-dimensional discrete time scale system (functional coefficient nonlinear autoregressive model).

The organization of this paper is as follows. In section 2, a stochastic discrete viral infection model with virus-driven proliferation of target cells is formulated. In section 3, the stability condition of the system are derived. The simulation is used in section 4, to discuss the analytical results, to show the effects of noise intensity on the dynamics of the system, and to give a numerical evidence about the chaotic behaviour of stochastic systems.

2. THE STOCHASTIC DISCRETE MODEL

Applying the forward Euler scheme to model (1.1) we obtain a general stochastic discrete viral infection model with virus-driven proliferation of target cells, in the following form:

$$\left\{\begin{array}{lcl} T_t &=& T_{t-1} + l(f(T_{t-1}, V_{t-1}) - k_1 h(T_{t-1}) g(V_{t-1})) + k\varepsilon_t \\ T_t^i &=& T_{t-1}^i + l(k_1 h(T_{t-1}) g(V_{t-1}) - \mu_2 p(T_{t-1}^i)) + k\eta_t \\ V_t &=& V_{t-1} + l(N\mu_2 p(T_{t-1}^i) - \mu_3 q(V_{t-1}) - k_2 h(T_{t-1}) g(V_{t-1})) + k\xi_t, \end{array}\right. \tag{2.1}$$

where l is the step size, the other functions are defined as in model (1.1) and $(\varepsilon_t, \eta_t, \xi_t)$ are assumed to be an *i.i.d.* white noise sequence conditional upon the history of the time series, which is denoted $\Omega_{t-1} = (T_{t-1}, T_{t-1}^i, V_{t-1})$ that is, $E[(\varepsilon_t, \eta_t, \xi_t)|\Omega_{t-1}] = 0$ and $E[\varepsilon_t^2|\Omega_{t-1}] = E[\eta_t^2|\Omega_{t-1}] = E[\xi_t^2|\Omega_{t-1}] = \sigma^2$, and k is a scalar parameter of the noise intensity. All parameters are assumed to be positive. In this paper we consider the system (2.1), where $f(T_{t-1}, V_{t-1}) = aT_{t-1} - T_{t-1}^2 - bT_{t-1}V_{t-1}$, $h(T_{t-1}) = T_{t-1}$, $g(V_{t-1}) = V_{t-1}$,$p(T_{t-1}^i) = T_{t-1}^i$, $q(V_{t-1}) = \alpha_2 V_{t-1} + \alpha_3 V_{t-1}^2$, and a, b,$\alpha 2$, and α_3 are positive parameters. Then the proposed system has the form:

$$\left\{\begin{array}{lcl} T_t &=& T_{t-1} + l(aT_{t-1} - T_{t-1}^2 - mT_{t-1}V_{t-1}) + k\varepsilon_t \\ T_t^i &=& T_{t-1}^i + l(k_1 T_{t-1}V_{t-1} - \mu_2 T_{t-1}^i) + k\eta_t \\ V_t &=& V_{t-1} + l(\alpha_1 T_{t-1}^i - \alpha_2 V_{t-1} - \alpha_3 V_{t-1}^2) - k_2 T_{t-1}V_{t-1}) + k\xi_t, \end{array}\right. \tag{2.2}$$

where $m = b + k1$, and $\alpha_1 = N\mu_2$.

3. THE SKELETON

In this section we study the chaotic behaviour of the free noise system (2.2) caused by the change of time step. Where $k = 0$, the system (2.2) becomes

$$\left\{\begin{array}{lcl} T_t &=& T_{t-1} + l(aT_{t-1} - T_{t-1}^2 - mT_{t-1}V_{t-1}) \\ T_t^i &=& T_{t-1}^i + l(k_1 T_{t-1}V_{t-1} - \mu_2 T_{t-1}^i) \\ V_t &=& V_{t-1} + l(\alpha_1 T_{t-1}^i - \alpha_2 V_{t-1} - \alpha_3 V_{t-1}^2) - k_2 T_{t-1}V_{t-1}). \end{array}\right. \tag{3.1}$$

Equilibria of the system (3.1) are derived in the following.

Lemma 3.1. The equilibria of the system (3.1), are $E_0 = (0, 0, 0)$, $E_1 = (a, 0, 0)$, $E_2 = (0, 0, -\frac{\alpha_3}{\alpha_2})$ and $E_3 = (a - m\alpha, \frac{b\alpha}{\mu_2}(a - m\alpha), \alpha)$, is a positive interior equilibrium point for $\alpha = \frac{a\mu_2 k_2 + \mu_2\alpha_2 - a\alpha_1 k1}{m\mu_2 k_2 - m\alpha_1 k_1 - \alpha_3\mu_3} > 0$ and $a > b\alpha$.

Proof. The equilibria of the system (3.1) are obtained as the solution of the algebraic system:

$$\left\{\begin{array}{lcl} T &=& T + l(aT - T^2 - mTV) \\ T^i &=& T^i + l(k_1 TV - \mu_2 T^i) \\ V &=& V + l(\alpha_1 T^i - \alpha_2 V - \alpha_3 V^2) - k_2 TV \end{array}\right. \tag{3.2}$$

which is obtained by setting $T_t = T_{t-1} = T$, $T_t^i = T_{t-1}^i = T^i$ and $V_t = V_{t-1} = V$ in (3.1), it is easy to get the results.

Now, we study the stability of these equilibria of model (3.1). The local stability analysis of the system (3.1) can be studied by computing the variation matrix corresponding to each equilibrium. The variation matrix of the system at state variable is given by

$$J(T, T^i, V) = \begin{pmatrix} \varphi_1 & 0 & -lmT \\ lk_1V & 1 - l\mu_2 & lk1T, \\ lk_2V & l\alpha_1 & \varphi_2 \end{pmatrix} \tag{3.3}$$

where, $\varphi_1 = 1 + l(a - 2T - mV)$ and $\varphi_2 = 1 - l(\alpha - 2 + 2\alpha_3 V + k_2 T)$

For the local stability of E_0, we have the following result.

Theorem 3.1. The following conclusions hold.
$A1$) If $l > \min\{\frac{2}{\mu_2}, \frac{2}{\alpha_2}\}$, then the equilibrium E_0 is a saddle point.
$A2$) If $l > \max\{\frac{2}{\mu_2}, \frac{2}{\alpha_2}\}$, then E_0 is a source.
$A3$) If $l = \frac{2}{\mu_2}$ or $l = \frac{2}{\alpha_2}$, then the equilibrium E_0 is non-hyperbolic.

Proof. In order to prove this result, we estimate the eigenvalues of Jacobian matrix at E_0. The Jacobian matrix for E_0 is

$$J(E_0) = \begin{pmatrix} 1 + la & 0 & 0 \\ 0 & 1 - l\mu_2 & 0 \\ 0 & l\alpha_1 & 1 - l\alpha_1 \end{pmatrix}.$$

Hence the eigenvalues of $J(E_0)$ are $\omega_1 = 1 + la$,$\omega_2 = 1 - l\mu_2$ and $\omega_3 = 1 - l\alpha_2$, and since all parameters are positive, we have $|\omega_1| > 1$. Let $l > \min\{\frac{2}{\mu_2}, \frac{2}{\alpha_2}\}$, then one of the other eigenvalues has an absolute value less than unit and the other has an absolute value greater than unit, which completes the proof of $(A1)$. It is easy to get $(A2)$ and $(A3)$.

For the local stability of E_1, we have the following result.

Theorem 3.2. If $ak_2 + \mu_2 + \alpha_2 > \sqrt{\beta_1}$ and $a^2k_2^2 + 2a\alpha_2k_2 + 4\alpha_1k_1a + \alpha_2^2 + \mu_2^2 > 2a\mu_2k_2 + 2\alpha_2\mu_2\alpha$, then
$H1$) E_1 is asymptotically stable if $0 < l < \min\{\beta_2, \beta_3\}$,
$H2$) E_1 is a saddle if $\min\{\beta_2, \beta_3\} < l < \max\{\beta_2, \beta_3\}$,
$H3$) E_1 is source if $l > \max\{\beta_2, \beta_3\}$,
$H4$) E_1 is non-hyperbolic if $l = \beta_2$, or β_3,
where $\beta_1 = a^2k_2^2 + 2a\alpha_2k_2 - 2a\mu_2k_2 + 4\alpha_1k_1a + \alpha_2^2 - 2\alpha_2\mu_2 + \mu_2^2$, $\beta_2 = \frac{2}{a}$, and $\beta_3 = \frac{4}{ak_2+\mu_2+\alpha_2+\sqrt{\beta_1}}$.

Proof. The Jacobian matrix (3.3) at E_1 has the form

$$J(E_1) = \begin{pmatrix} 1-la & 0 & -lma \\ 0 & 1-l\mu_2 & lak_1 \\ 0 & l\alpha_1 & 1-l[\alpha_2+ak_2] \end{pmatrix}.$$

The eigenvalues of $J(E_1)$ are $\omega_1 = 1-la$, and $\omega_{2,3} = (1/2)[2-l(ak_2+\mu_2+\alpha_2 \mp \sqrt{\beta_1})]$. After some calculations, we obtain the results.

For the local stability of E_2, we have the following result.

Theorem 3.3. The following conclusions hold.

$M1$) If $0 < l < \frac{2}{\mu_2}$, then E_2 is a saddle point,

$M2$) If $l > \frac{2}{\mu_2}$, then E_2 is a source,

$M3$) if $l = \frac{2}{\mu_2}$, then E_2 is non-hyperbolic.

Proof. We can get the proof by same structure in the previous theorem.

For local stability of E_3 we have the following result.

Theorem 3.4 The equilibrium point E_3 is asymptotically stable iff $A > 0$, $B > 0$, $C > 0$, and $AB > C$, where $A = l\beta + l\mu_2 + l\theta - 3$, $B = (l\beta-1)(l\mu_2-1)+(l\theta-1)(l\beta+l\mu_2-2)-l^2\beta\alpha_1k_1-l^2m\alpha\beta k_2$, $C = l\alpha_1(l\beta k_1(l\mu_2-1)+l^2m\alpha\beta k_1)-l^2\rho+(l\beta-1)(l\mu_2-1)(l\theta-1)$, $\theta = \alpha_2+2\alpha\alpha_3+\beta k_2$, and $\rho = (\beta\alpha_1k_1+m\alpha\beta k_2)(l\beta+l\mu_2-2)-m\alpha\beta k_2(l\beta-1)$.

Proof. The proof can be obtained by the same procedure in the previous theorem and applying Jury criterion, [33].

4. NUMERICAL SIMULATION

The main objectives of this section are: to introduce a numerical evidence about the chaotic behaviour of the system (2.2); to discuss the interrelationship between the dynamics of the skeleton and the complex dynamics of the stochastic system; and to investigate the changes of parameters and noise intensity effects on the dynamics of the stochastic system which may be regarded as an indicator of the chaotic behaviour of the asymptotic marginal distribution of the state variables. Throughout this section, we consider the initial point $(x_0, y_0, z_0) = (0.4, 0.3, 0.2)$, and other parameters $a = 0.3, m = 5, k_1 = 0.3, \mu_2 = 0.2, \alpha_1 = 0.3, \alpha_2 = 4, \alpha_3 = 6$, and $k_2 = 0.2$.

4.1. **Deterministic system.** In this subsection the qualitative behavior of the solution of the nonlinear system (3.1) is investigate. Various numerical results are presented here to show the chaoticity including its, bifurcation diagrams, Lyapunov exponents, and fractal dimension. Bifurcation diagrams of the system (3.1) are plotted on the interval $0.1 \le l \le 0.7$ in Figs. 1(a), (b), and (c). It is corresponding maximum Lyapunov exponent is given in Fig. 1(d). A positiveness of this exponent for $l > l^* \simeq 0.491$ confirms the chaotic character of attractors in this parametrical zone, [4] (here, the value $l^* \simeq 0.491$ is a tangent bifurcation point). To show the chaotic behaviour of

the system, phase portraits are given for different values of l in Fig. 2. For the given parameters the only positive equilibrium point is, $E_1^* = (0.3, 0, 0)$ which is attracting point for $0.1 < l \leq 0.491$ as we can see in Fig. 2(a). Fig. 2(b) show the period-two orbit in the parameter zone $0.491 < l \leq 0.601$. The period-four orbit in the parameter zone $0.601 < l \leq 0.624$ is clear in Fig. 2(c). The period-eight orbit in the parameter zone $0.624 < l \leq 0.63$ is clear in Fig. 3(c). The chaotic attractor for $0.63 < l \leq 0.7$ is clear in Fig. 2(d). Which means that the system (3.1) undergoes a discrete Hopf bifurcation. One of the commonly used characteristics for classifying and quantifying the chaoticity of a dynamical system is Lyapunov dimension, [23, 39]. Via simulation we get three Lyapunov exponents $\lambda_1 = 1.490 > N_2 = -0.136 > N_3 = -2.896$ for $l = 0.639$, which means that $d_L \simeq 2.46$. Therefor the system (3.1) exhibits a fractal structure and its attractor has a fractal dimension which is chaotic behaviour.

4.2. **Stochastic Model.** In this subsection, we consider a stochastic system forced by additive noise (2.2), where ε_t, η_t and ξ_t are uncorrelated Gaussian random processes with parameters $E\varepsilon_t = E\eta_t = E\xi_t = 0$, $E\varepsilon_t^2 = E\eta_t^2 = E\xi_t^2 = 1$ and k is a scalar parameter of the noise intensity. The main objectives of this subsection are: to give a numerical evidence about the interrelationship between the dynamics of the stochastic system and its skeleton; to discuss the phenomenon of noise-induced intermittency; and to investigate the changes of parameters and noise intensity effects on the asymptotic marginal distribution of the state variables, which may be regarded as an indicator of stochastic chaotic distribution of the system. We study a behavior of this stochastic system for different values of parameters l and k. In Fig. 3, bifurcations diagrams of the system (2.2) are plotted on the interval $0.1 \leq l \leq 0.7$ for three values of the noise intensity $k = 0.0001, 0.0003$, and 0.0006. Maximum Lyapunov exponents corresponding to each value of noise intensity are given in Fig. (4)(a), (b) and (c) respectively. By comparing Figs. 1 and 3, we can see how noise deforms the deterministic attractor. The dynamical characteristics are also changed (compare Lyapunov exponents in Figs. 1(d) and 4). As noise intensity increases, a border between order and chaos moves to the left, see Fig. 4. To follow the dynamics of the system (2.2), time series, phase portraits and stochastic attractors are plotted for different values of l and k. For $l = 0.485$, with low noise $k = 0.0001$, the states (x_t, y_t, z_t) oscillate with low amplitude around the stable deterministic equilibrium E_1^*. Random states are concentrated near the stable deterministic equilibrium, see Figs. $5(a) - 5(c)$ and $10(a)$. With high noise $k = 0.0006$, we can observe the stochastic oscillations of large amplitude and the increase of the dispersion, see Figs. $5(d) - 5(f)$, $10(b)$ and $11(a) - 11(c)$. For $l = 0.495$, the stochastic oscillations of large amplitude around the deterministic period-two orbit $(0.28516, 0.00078, -0.04050)$ and $(0.31584, -0.00101, 0.03608)$, can be observed even though for low noise intensity $k = 0.0001$, see Fig. 6. In this case, the stochastic system (2.2) exhibits a coexistence of two different dynamical regimes even if the system

(3.1) has a stable equilibrium only. This type of dynamics of the system (2.2) can be determined as a noise-induced intermittency, [2, 17], see Figs. $6(a)-6(c)$, $10(c)$, $10(d)$ and $11(d)$-$11(f)$. For $l = 0.616$, the stochastic oscillations of large amplitude around the deterministic period-four orbit $(0.18882, 0.00396, -0.31418)$, $(0.38447, -0.00749, 0.10317)$, $(0.24229, 0.00076, -0.19666)$, and $(0.39766, -0.00814, 0.15098)$ can be observed even though for low noise intensity $k = 0.0001$, see Figs. 7; $10(e)$, $10(f)$ and $11(g)$-$11(i)$. In this case, the stochastic system (2.2) exhibits a coexistence of four different dynamical regimes even if the system (3.1) has a stable equilibrium only. The stochastic chaotic behaviour can be observed for $l = 0.640 and l = 0.670$, even though for low noise intensity $k = 0.0001$, see Figs. 8, 9; $10(g) - 10(j)$; and $11(j) - 11(o)$. For stochastic dynamic characteristics, the dependence on noise level is illustrated in Fig. 12 for $l = 0.490$ and $l = 0.4909$. To investigate the changes of parameters and noise intensity effects on the asymptotic marginal distribution of the state variables, we discuss it for different values of l and k. For $l = 0.485$, and $0 \leq k \leq 0.0006$ the marginal distribution of the state variables is asymptotically normal, with mean $E_1^* = (0.3, 0, 0)$, which we may call it a stable distribution see Figs. $13(a) - 13(c)$, the sample statistics are given in Table 1. As the control parameter l increases the asymptotic distribution split into two regimes, see Figs. $13(d)-13(f)$ and Table 2, for $l = 0.495$, then into four regimes, see Figs. $13(g)-13(i)$ and Table 3, for $l = 0.616$, and so on until it reaches what we may call it chaotic distribution, see Figs. $13(j)-13(o)$, and Tables 4 and 5, for $l = 0.640$ and $l = 0.670$, respectively. This phenomenon may be regarded as an indicator of stochastic chaotic behaviour.

5. CONCLUSION

The current paper has presented a new stochastic discrete chaotic viral infection model with virus-driven proliferation of target cells. The model shows rich and varied dynamics and chaos. Local stability of equilibria have been discussed. The results show that, for certain parametric restrictions there is a unique interior equilibrium point which is locally stable. When the time step parameter passes a critical value the attractor is a period-2 cycle. As the time step parameter increases, both branches split simultaneously, yielding a period-4 cycle. This splitting is the period-doubling bifurcation. A cascade of further period-doubling occurs as the time step parameter increases, yielding period-8, period-16, and so on until the map becomes chaotic and the attractor changes from a finite to an infinite set of points. The results referred to that there is a closed relationship between the time step parameter changes and the distribution of the states of the stochastic system. The remarkable feature of the dynamics of the model considered here is that small noises generate large-amplitude chaotic oscillation. The asymptotic distribution of the state variables is used as an indicator of the chaotic behaviour of stochastic systems, which still an open problem.

ACKNOWLEDGMENTS

I would like to thank professor G. S. Ladde for his carefully reading this paper and recommending it for publication in NPSC journal. I would like to thank professor M. Sambandham and referees for their efforts in reading this paper.

REFERENCES

[1] E. Avila-Vales, N. Chan-Chi, G.E. Garcia-Almeida and C. Vargas-De-Le, Stability and Hopf bifurcation in a delayed viral infection model with mitosis transmission, *Appl. Math. and Comput.*, 259:293–312, 2015.

[2] I. Bashkirtseva and L. Ryashko, Stochastic sensitivity analysis of noise-induced intermittency and transition to chaos in one-dimensional discrete-time systems, *Physica A*, 392:295–306, 2013.

[3] D. Callaway and A. Perelson, HIV-1 infection and low steady state viral loads, *Bull. Math. Biol.*, 64:29–64, 2002.

[4] J. H. E. Cartwright, Nonlinear stiffness, Lyapunov exponents, and attractor dimension, *Phys. Lett. A*, 264:298–304, 1999.

[5] A. Cordero, F. Soleymani and J.R. Torregrosa, Dynamical analysis of iterative methods for nonlinear systems or how to deal with the dimension?, *Appl. Math. and Comput*, 244:398–412, 2014.

[6] R.V. Culshaw and S.G. Ruan, A delay-differential equation model of HIV infection of $CD4^+$ T-cells, *Math. Biosci.*, 165:27–39, 2000.

[7] R.V. Culshaw, S.G. Ruan and G. Webb, A mathematical model of cell-to-cell spread of HIV-1 that includes a time delay, *J. Math. Biol.*, 46:425–444, 2003.

[8] R.L. Devaney, *An Introduction to Chaotic Dynamical Systems*, Addison-Wesely Reading, 1989.

[9] N.M. Dixit and A.S. Perelson, Complex patterns of viral load decay under antiretroviral therapy: influence of pharmacokineticsand intracellular delay, *J. Theor. Biol.*, 226:95–109, 2004.

[10] N.H. Du and V.H. Sam, Dynamics of a stochastic Lotka-Volterra model perturbed by white noise, *J. Math. Anal. Appl.*, 324:82–497, 2006.

[11] T. Dumrongpokaphan, Y. Lenbury, R. Ouncharoen and Y.S. Xu, An intracellular delay- differential equation model of the HIV infection and immune control, *Math. Model. Nat. Phenom. Epidemiol.*, 2:75–99, 2007.

[12] A. Elhassanein, On the complex dynamics of functional-coefficients nonlinear autoregressive time series models, *Communications in Statistics: Simulation and Computation*, DOI:10.1080/03610918.2015.1044615

[13] A. Elhassanein, Complex dynamics of logistic self-exciting threshold autoregressive model, *J. Comput. Theor. Nanosci.*, 12(4):542–548, 2015.

[14] A. Elhassanein, On the control of forced process feedback nonlinear autoregressive model, *J. Comput. Theor. Nanosci.*, 12(8):1519–1526, 2015.

[15] A. Elhassanein, Complex dynamics of a stochastic discrete modified Leslie-Gower predator-prey model with Michaelis-Menten type prey harvesting, *Computational Ecology and Software*, 4:116–128, 2014.

[16] A. Elhassanein, Complex dynamics of a forced discretized version of the Mackey-Glass delay differential equation, *Discrete Contin. Dyn. Syst. Ser. B*, 20(1):93–105, 2015.

[17] A. Elhassanein, Complex dynamics of forced LSTAR model with delay, *Dynamics of Continuous, Discrete and Impulsive Systems*, 21:435–447, 2014.

[18] A.A. Elsadany, Dynamical complexities in a discrete-time food chain, *Computational Ecology and Software*, 2:124–139, 2012.

[19] M.A. Ghazal and A. Elhassanein, Dynamics of EXPAR models for high frequency data, *Int. J. Appl. Math. Stat.*, 14:88–96, 2009.

[20] Z. Han and J. Zhao, Stochastic SIRS model under regime switching, *Nonlinear Analysis: Real World Applications*, 14:352–364, 2013.

[21] C. Ji, D. Jiang and X. Li, Qualitative analysis of a stochastic ratio-dependent predator-prey system, *J. Comput. Appl. Math.*, 235:1326–1341, 2011.

[22] D. Jiang, N. Shi and X. Li, Global stability and stochastic permanence of a non-autonomous logistic equation with random perturbation, *J. Math. Anal. Appl.*, 340:588–597, 2008.

[23] J.L. Kaplan and Y.A. Yorke, A regime observed in a fluid flow model of Lorenz, *Comm. Math. Phys.*, 67:93–108, 1979.

[24] P. Katri and S.G. Ruan, Dynamics of human T-cell lym-photropic virus I (HTLV-I) infection of $CD4^+$ T-cells, *C. R. Biol.*, 327:1009–1016, 2004.

[25] N. Kazantzis and V. Kazantzi, Reduced-order state reconstruction for nonlinear dynamical systems in the presence of model uncertainty, *Appl. Math. and Comput.*, 218(23):11708–11718, 2012.

[26] D. Kirschner, Using mathematics to understand HIV immune dynamics, *Notices of the AMS*, 43:191–202, 1996.

[27] X. Li, X. Fu and R. Rakkiyappan, Delay-dependent stability analysis for a class of dynamical systems with leakage delay and nonlinear perturbations, *Appl. Math. and Comput.*, 226:10–19, 2014.

[28] X. Li and X. Mao, Population dynamical behavior of non-autonomous Lotka-Volterra competitive system with random perturbation, *Discrete Contin Dyn. Syst.*, 24:523–545, 2009.

[29] M.Y. Li and H. Shu, Global dynamics of an in-host viral model with intracellular delay, *Bulletin of Mathematical Biology*, 72:1492–1505, 2010.

[30] D. Liu, W. Xu and Y. Xu, Noise-induced chaos in the elastic forced oscillators with real-power damping force, *Nonlinear Dyn.*, 71:457–467, 2013.

[31] X. Mao, G. Marion and E. Renshaw, Environmental Brownian noise suppresses explosions in population dynamics, *Stoch. Process Appl.*, 97:95–110, 2002.

[32] M.A. Nowak and R.M. May, *Virus Dynamics*, Cambridge University Press, Cambridge, 2000.

[33] P.C. Parks and V. Hahn, *Stability Theory*, Prentice Hall, New York, 1992.

[34] H. Shu and L. Wang, Global stability and backeard bifurcation of a general viral infection model with virus-driven proliferation of target cells, *Discrete Contin. Dyn. Syst. Ser. B*, 19:1749–1768, 2014.

[35] H.S. Steven, *Nonlinear Dynamics and Chaos: with Applications to Physics, Biology, Chemistry and Engineering*, Perseus Books Publishing, L. L. C., 1994.

[36] L. Wang and S. Ellermeyer, HIV infection and $CD4^+$ T cell dynamics, *Discrete Contin. Dyn. Syst. Ser. B*, 6:1417–1430, 2006.

[37] L. Wang and M.Y. Li, Mathematical analysis of the global dynamics of a model for HIV infection of $CD4^+$ T cells, *Math. Biosci.*, 200:44–57, 2006.

[38] C. Zhu and G. Yin, On competitive Lotka-Volterra model in random environments, *J. Math. Anal. Appl.*, 357:154–170, 2009.

[39] C.R. Zhu and K.Q. Lan, Phase portraits, Hopf-bifurcations and limit cycles of Leslie-Gower predator-prey systems with harvesting rates, *Discrete Contin. Dyn. Syst. Ser. B*, 14:289–306, 2010.

TABLE 1. Sample statistics of the variable state (x_t, y_t, z_t), with initial values $(x_0, y_0, z_0) = (0.4, 0.3, 0.2)$, for $l = 0.475$ and $k \in [0.0, 0.0006]$, where $a = 0.3, m = 5, k_1 = 0.3, \mu_2 = 0.2, \alpha_1 = 0.3, \alpha_2 = 4, \alpha_3 = 6$, and $k_2 = 0.2$.

$l = 0.485$	Mean	Median	St.D.	Skewness	Kurtosis
x_t	0.300	0.300	0.000	0.06	2.34
y_t	0.000	0.000	0.000	0.08	2.59
z_t	0.000	0.000	0.001	-0.03	2.33

TABLE 2. Sample statistics of the variable state (x_t, y_t, z_t), with initial values $(x_0, y_0, z_0) = (0.4, 0.3, 0.2)$, for $l = 0.495$ and $k \in [0.0, 0.0006]$, where $a = 0.3, m = 5, k_1 = 0.3, \mu_2 = 0.2, \alpha_1 = 0.3, \alpha_2 = 4, \alpha_3 = 6$, and $k_2 = 0.2$.

$l = 0.495$	Mean	Median	St.D.	Skewness	Kurtosis
x_t	0.300	0.300	0.015	0.00	-1.98
y_t	0.000	0.000	0.001	-0.02	-0.11
z_t	-0.002	-0.001	0.038	0.00	-1.99

TABLE 3. Sample statistics of the variable state (x_t, y_t, z_t), with initial values $(x_0, y_0, z_0) = (0.4, 0.3, 0.2)$, for $l = 0.616$ and $k \in [0.0, 0.0006]$, where $a = 0.3, m = 5, k_1 = 0.3, \mu_2 = 0.2, \alpha_1 = 0.3, \alpha_2 = 4, \alpha_3 = 6$, and $k_2 = 0.2$.

$l = 0.616$	Mean	Median	St.D.	Skewness	Kurtosis
x_t	0.303	0.314	0.100	-0.12	-1.82
y_t	-0.003	-0.003	0.005	0.13	-1.74
z_t	-0.064	-0.044	0.196	-0.11	-1.80

TABLE 4. Sample statistics of the variable state (x_t, y_t, z_t), with initial values $(x_0, y_0, z_0) = (0.4, 0.3, 0.2)$, for $l = 0.64$ and $k \in [0.0, 0.0006]$, where $a = 0.3, m = 5, k_1 = 0.3, \mu_2 = 0.2, \alpha_1 = 0.3, \alpha_2 = 4, \alpha_3 = 6$, and $k_2 = 0.2$.

$l = 0.64$	Mean	Median	St.D.	Skewness	Kurtosis
x_t	0.303	0.332	0.095	-0.20	-1.73
y_t	-0.003	-0.005	0.006	0.21	-1.67
z_t	-0.071	-0.022	0.205	-0.18	-1.71

TABLE 5. Sample statistics of the variable state (x_t, y_t, z_t), with initial values $(x_0, y_0, z_0) = (0.4, 0.3, 0.2)$, for $l = 0.67$ and $k \in [0.0, 0.0006]$, where $a = 0.3, m = 5, k_1 = 0.3, \mu_2 = 0.2, \alpha_1 = 0.3, \alpha_2 = 4, \alpha_3 = 6$, and $k_2 = 0.2$.

$l = 0.67$	Mean	Median	St.D.	Skewness	Kurtosis
x_t	0.306	0.341	0.091	-0.65	-0.96
y_t	-0.003	-0.005	0.005	0.65	-0.90
z_t	-0.065	-0.016	0.197	-0.60	-0.88

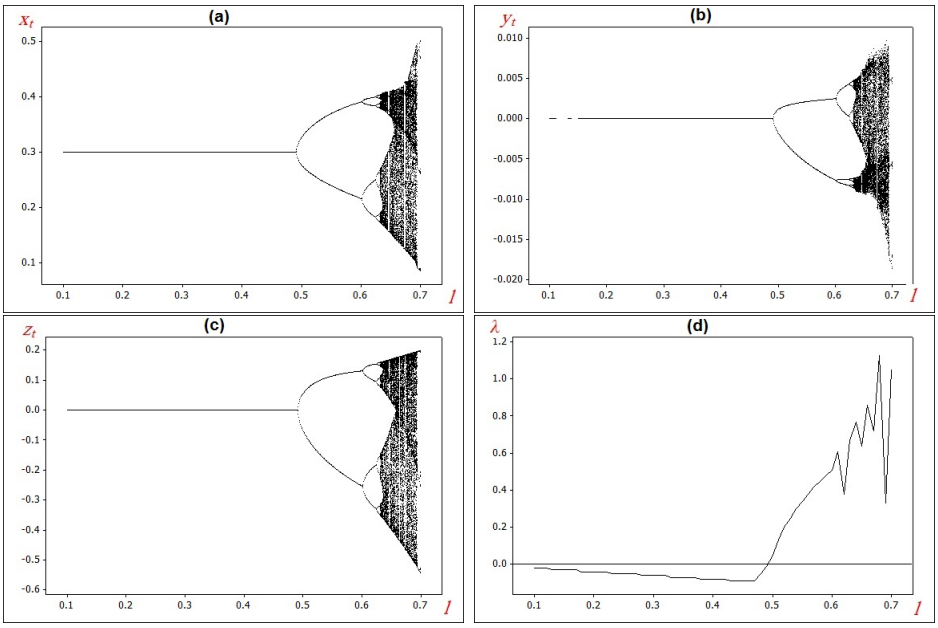

FIGURE 1. Bifurcation diagram of (3.1), for $0.1 \leq l \leq 0.7$ for initial point $(x_0, y_0, z_0) = (0.4, 0.3, 0.2)$ for: $(a)x_t$; $(b)y_t$; $(c)z_t$; (d) its corresponding Maximum Lyapunov exponents with $a = 0.3, m = 5, k_1 = 0.3, \mu_2 = 0.2, \alpha_1 = 0.3, \alpha_2 = 4, \alpha_3 = 6$, and $k_2 = 0.2$.

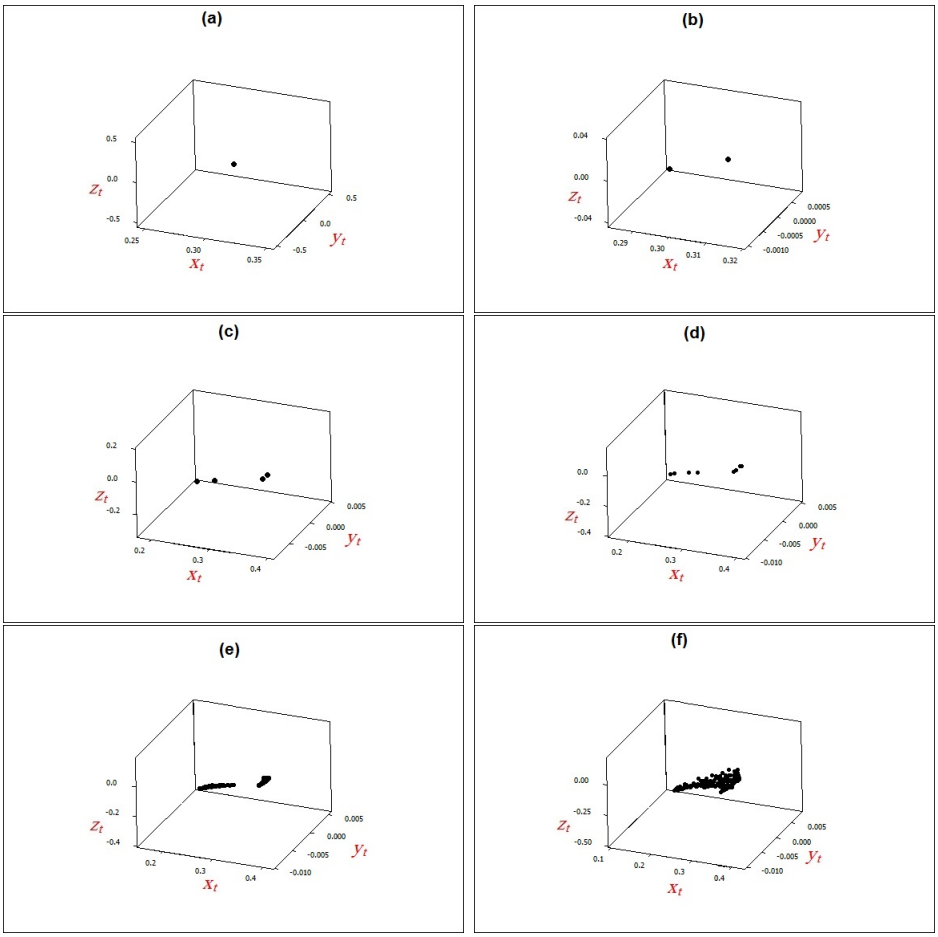

FIGURE 2. Phase portrait of the system (3.1) for: $(a)l = 0.490$; $(b)l = 0.495$; $(c)l = 0.616$; $(d)l = 0.630$; $(e)l = 0.640$; $(f)l = 0.670$ with $a = 0.3, m = 5, k_1 = 0.3, \mu_2 = 0.2, \alpha_1 = 0.3, \alpha_2 = 4, \alpha_3 = 6$, and $k_2 = 0.2$.

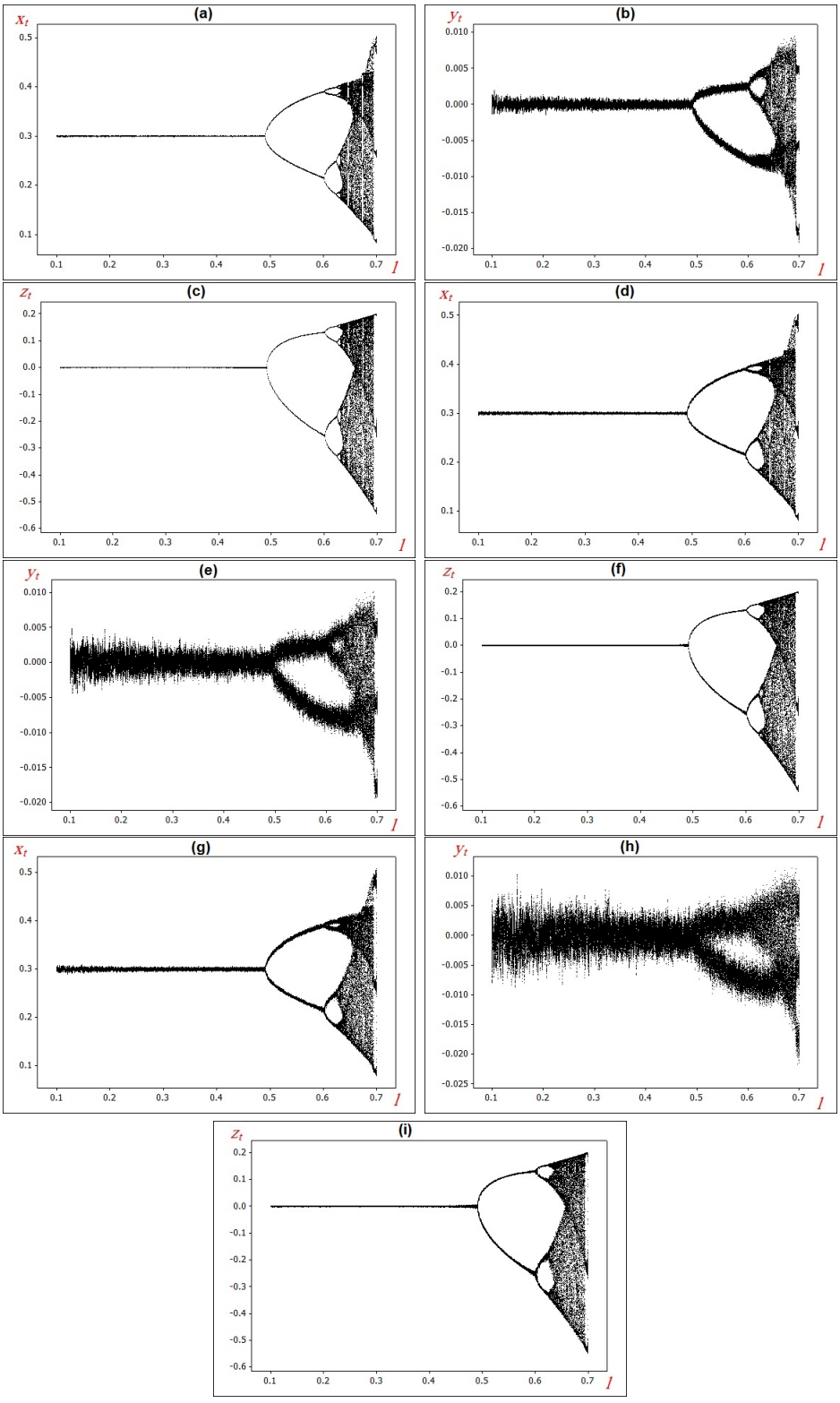

FIGURE 3. Bifurcation diagram of the stochastic model (2.2), with $0.1 \leq l \leq .7$ and the initial point $(x_0, y_0, z_0) = (0.4, 0.3, 0.2)$ for: $(a)x_t$; $(b)y_t$; $(c)z_t$, with $k = 0.0001$; $(d)x_t$; $(e)y_t$; $(f)z_t$, with $k = 0.0003$; $(g)x_t$; $(h)y_t$; $(i)z_t$, with $k = 0.0006$; where $a = 0.3, m = 5, k_1 = 0.3, \mu_2 = 0.2, \alpha_1 = 0.3, \alpha_2 = 4, \alpha_3 = 6$, and $k_2 = 0.2$.

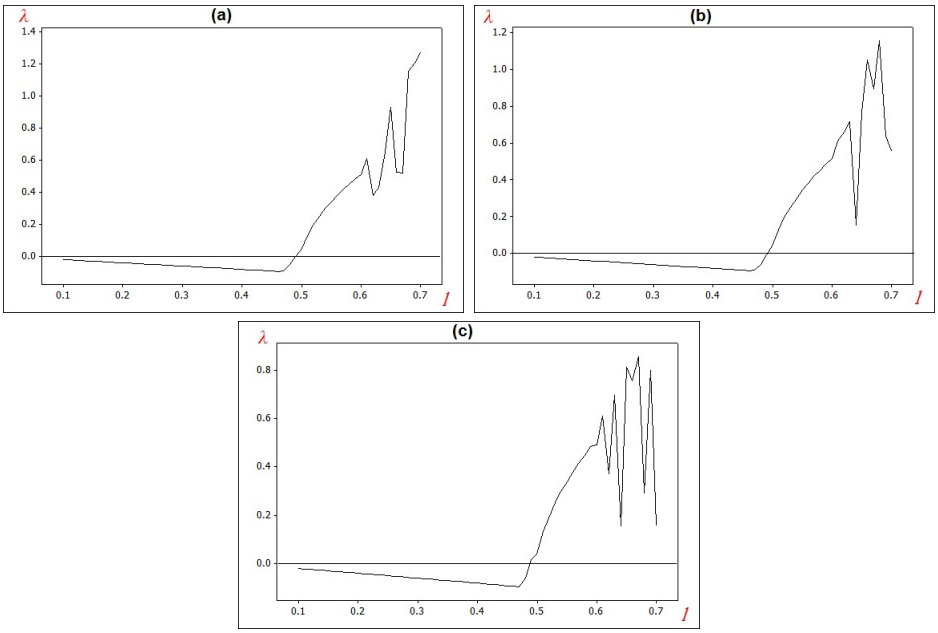

FIGURE 4. Lyapunov exponents of the stochastic model (2.2) with $l \in [0.1, 0.7]$ for: $(a)k = 0.0001$; $(b)k = 0.0003$; $(c)k = 0.0006$.

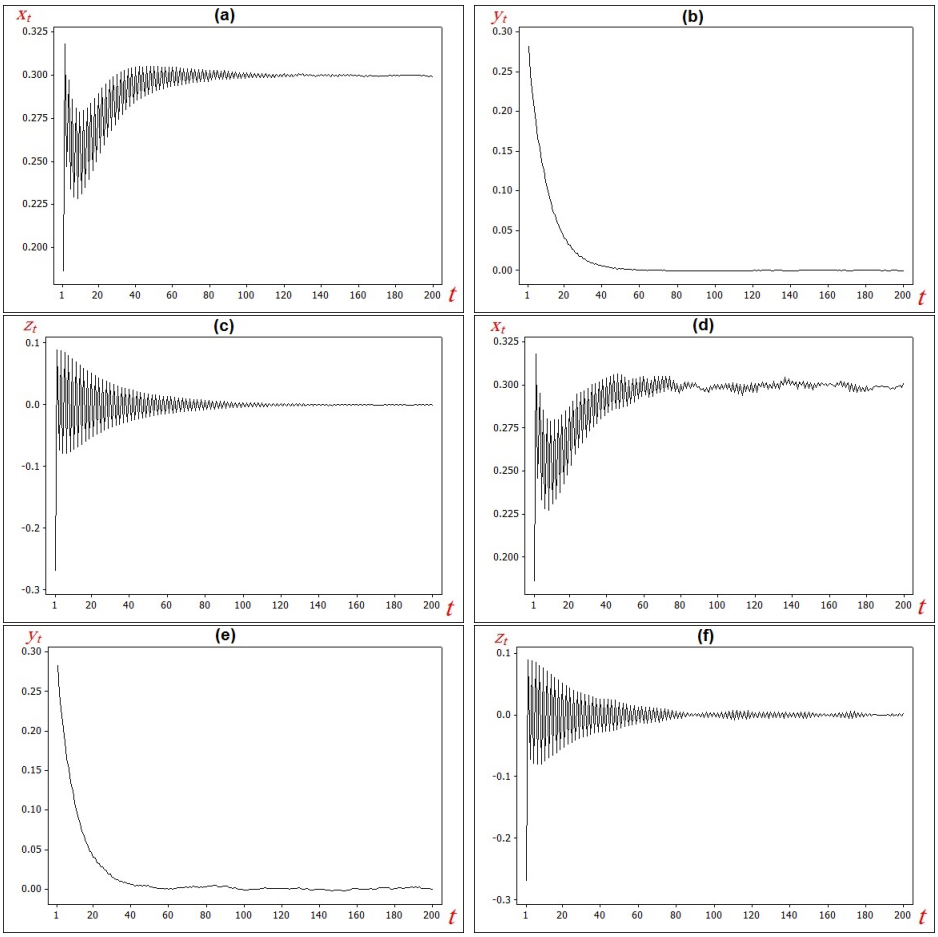

FIGURE 5. Time series of the stochastic model (2.2) with $l = 0.485$ and $k = 0.0001$ for: $(a)x_t$; $(b)y_t$; $(c)z_t$ and with $l = 0.485$ and $k = 0.0006$ for: $(d)x_t$; $(e)y_t$; $(f)z_t$, where $a = 0.3, m = 5, k_1 = 0.3, \mu_2 = 0.2, \alpha_1 = 0.3, \alpha_2 = 4, \alpha_3 = 6$, and $k_2 = 0.2$.

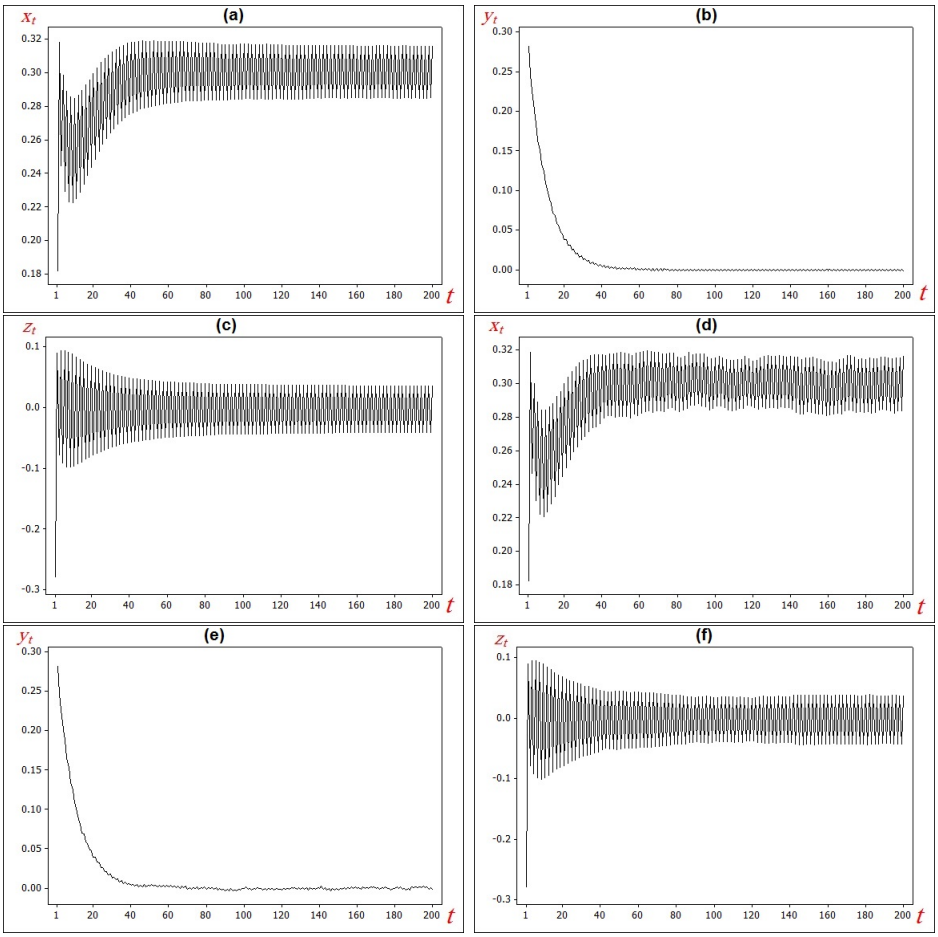

FIGURE 6. Time series of the stochastic model (2.2) with $l = 0.495$ and $k = 0.0001$ for: $(a)x_t$; $(b)y_t$; $(c)z_t$ and with $l = 0.495$ and $k = 0.0006$ for: $(d)x_t$; $(e)y_t$; $(f)z_t$, where $a = 0.3, m = 5, k_1 = 0.3, \mu_2 = 0.2, \alpha_1 = 0.3, \alpha_2 = 4, \alpha_3 = 6$, and $k_2 = 0.2$.

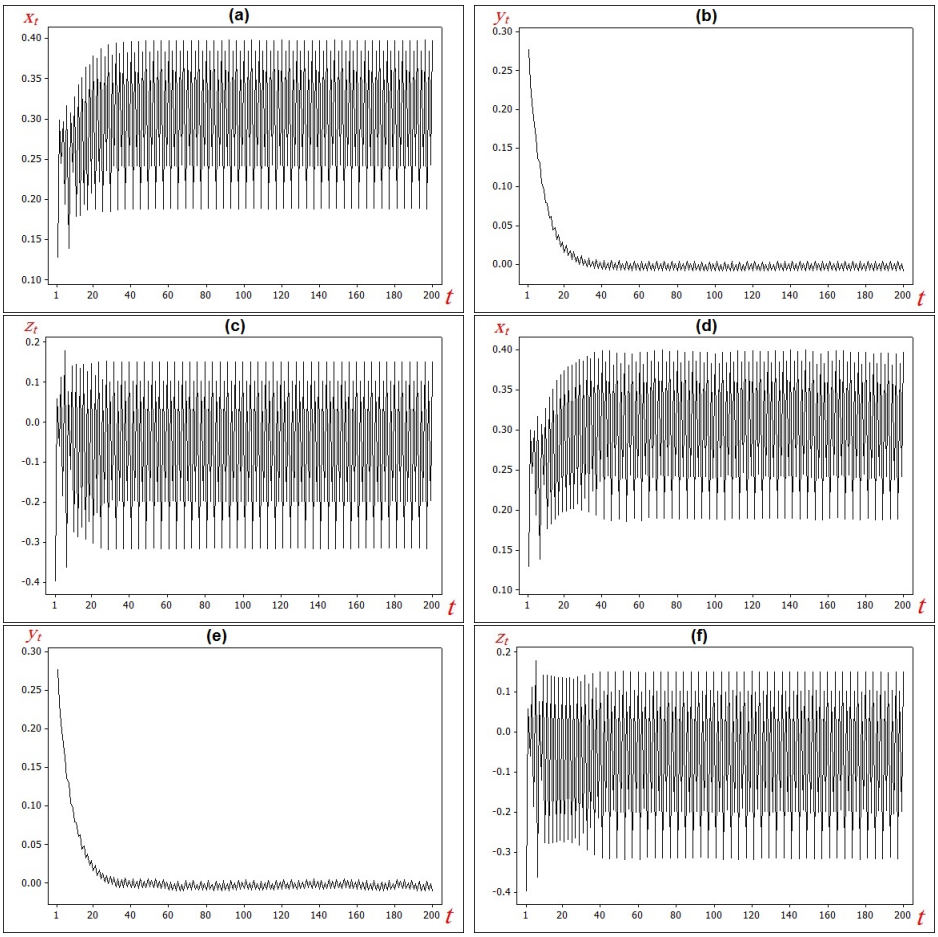

FIGURE 7. Time series of the stochastic model (2.2) with $l = 0.616$ and $k = 0.0001$ for: $(a)x_t$; $(b)y_t$; $(c)z_t$ and with $l = 0.616$ and $k = 0.0006$ for: $(d)x_t$; $(e)y_t$; $(f)z_t$, where $a = 0.3, m = 5, k_1 = 0.3, \mu_2 = 0.2, \alpha_1 = 0.3, \alpha_2 = 4, \alpha_3 = 6$, and $k_2 = 0.2$.

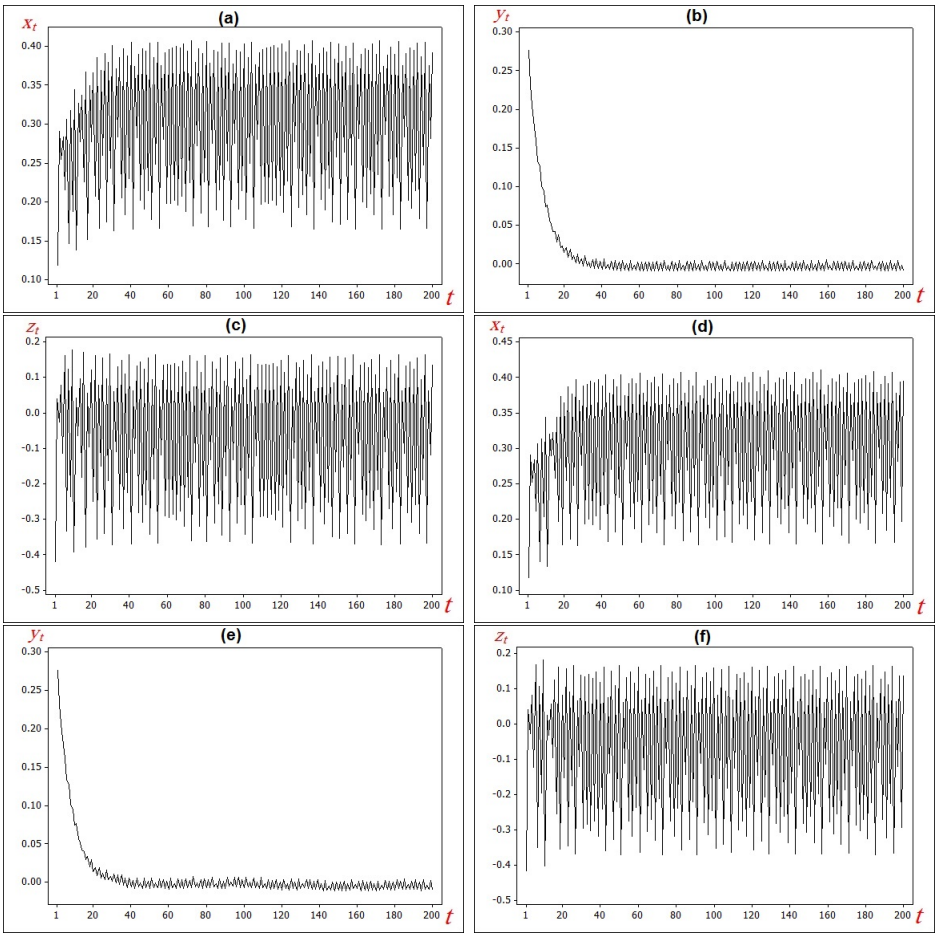

FIGURE 8. Time series of the stochastic model (2.2) with $l = 0.640$ and $k = 0.0001$ for: $(a)x_t$; $(b)y_t$; $(c)z_t$ and with $l = 0.640$ and $k = 0.0006$ for: $(d)x_t$; $(e)y_t$; $(f)z_t$, where $a = 0.3, m = 5, k_1 = 0.3, \mu_2 = 0.2, \alpha_1 = 0.3, \alpha_2 = 4, \alpha_3 = 6$, and $k_2 = 0.2$.

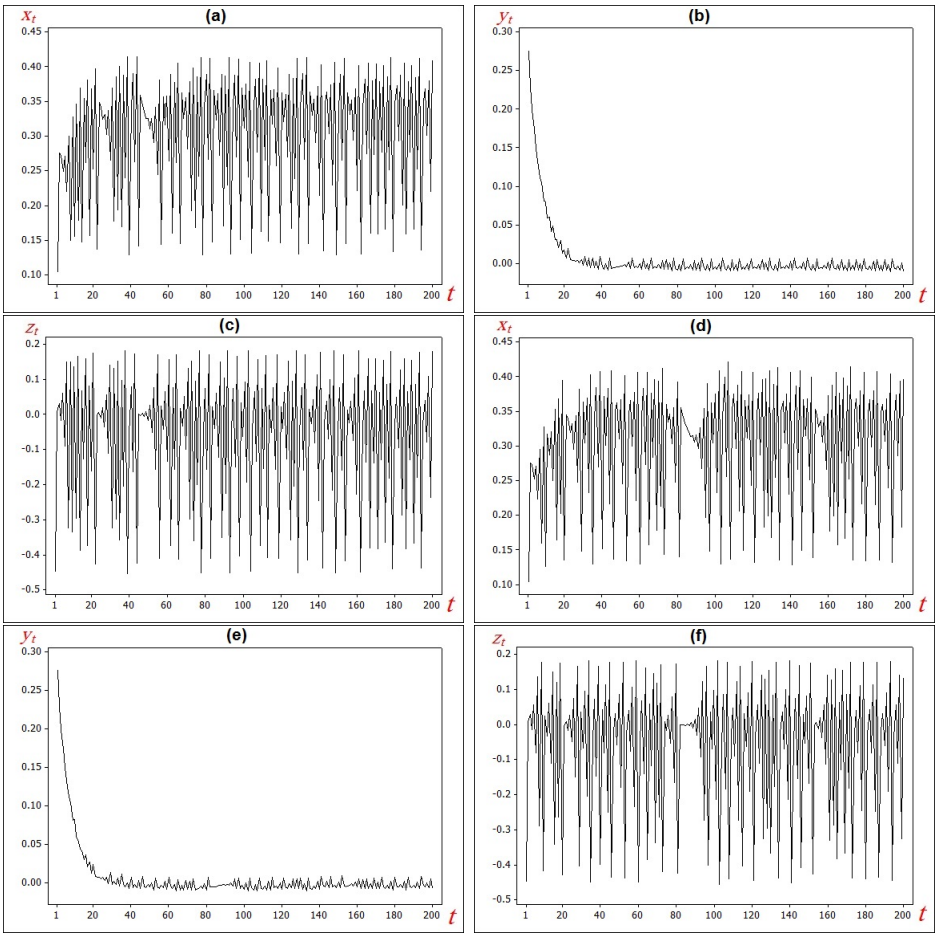

FIGURE 9. Time series of the stochastic model (2.2) with $l = 0.670$ and $k = 0.0001$ for: $(a)x_t$; $(b)y_t$; $(c)z_t$ and with $l = 0.67$ and $k = 0.0006$ for: $(d)x_t$; $(e)y_t$; $(f)z_t$, where $a = 0.3, m = 5, k_1 = 0.3, \mu_2 = 0.2, \alpha_1 = 0.3, \alpha_2 = 4, \alpha_3 = 6$, and $k_2 = 0.2$.

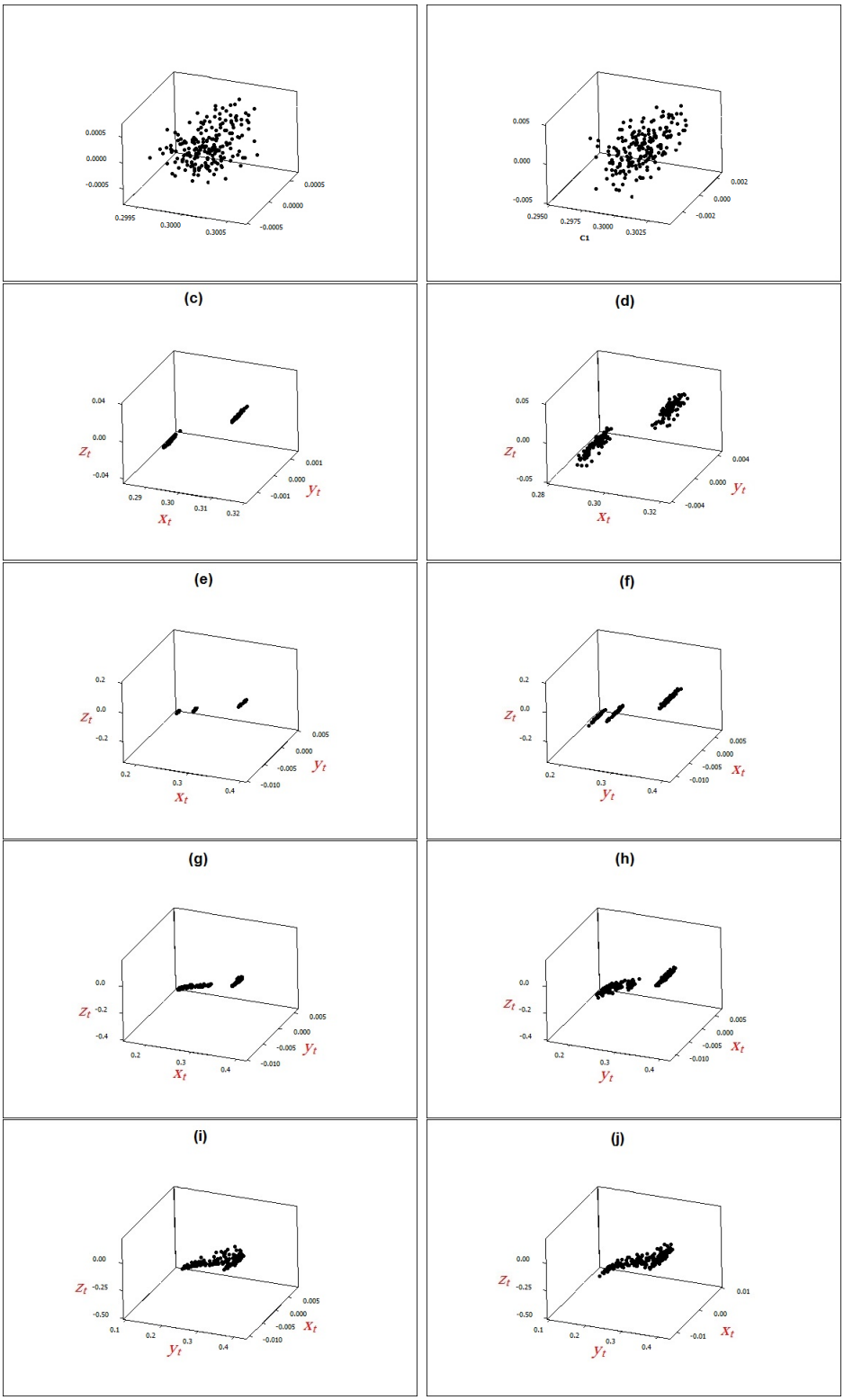

FIGURE 10. Phase portrait of the stochastic system (3.1) for: $(a)l = 0.490$ and $k = 0.0001$; $(b)l = 0.485$ and $k = 0.0006$; $(c)l = 0.495$ and $k = 0.0001$; $(d)l = 0.495$ and $k = 0.0006$; $(e)l = 0.616$ and $k = 0.0001$; $(f)l = 0.616$ and $k = 0.0006$; (g) $l = 0.640$ and $k = 0.0001$; $(h)l = 0.640$ and $k = 0.0006$; $(i) = 0.670$ and $k = 0.0001$; $(b)l = 0.670$ and $k = 0.0006$, with $a = 0.3, m = 5, k_1 = 0.3, \mu_2 = 0.2, \alpha_1 = 0.3, \alpha_2 = 4, \alpha_3 = 6$, and $k_2 = 0.2$.

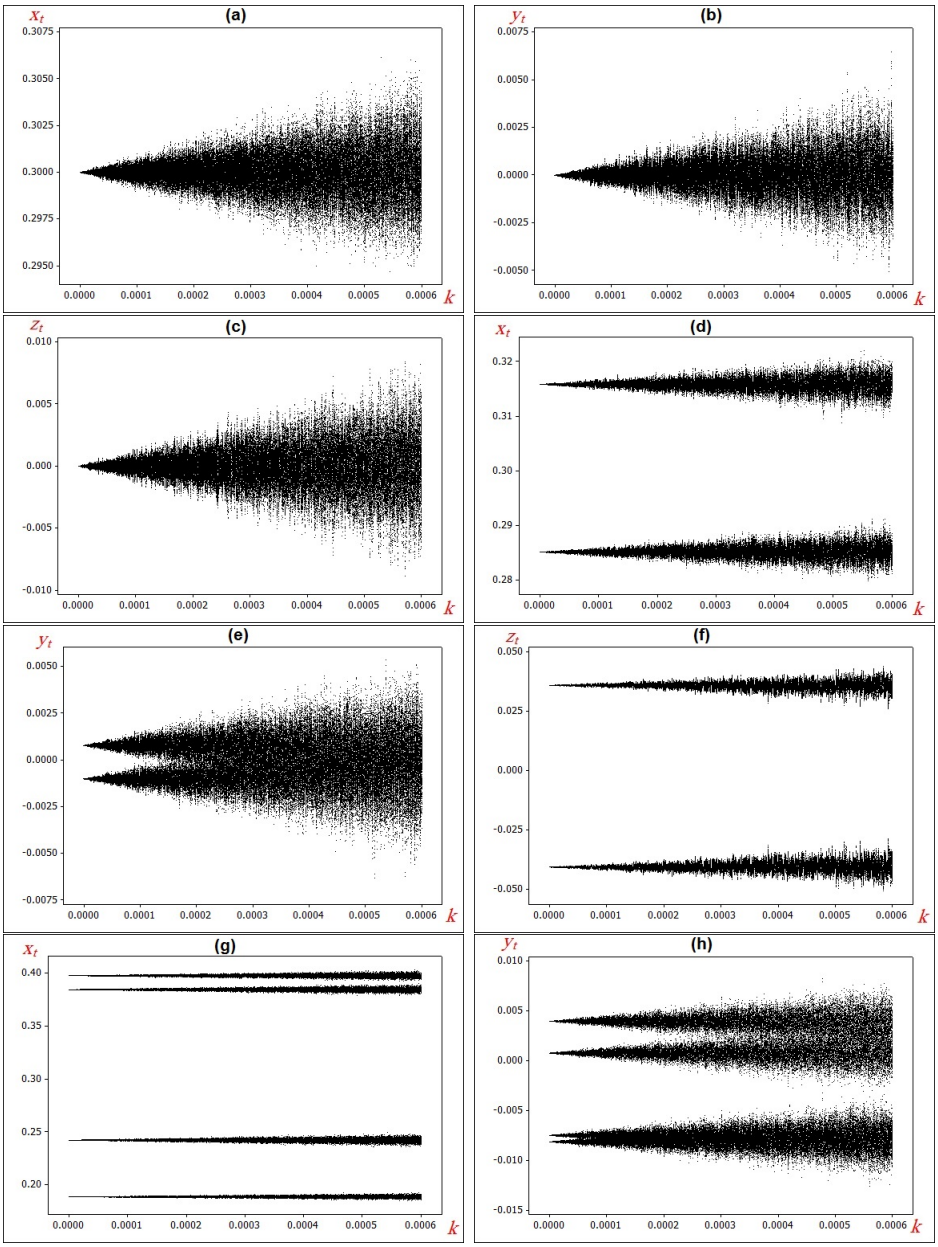

FIGURE 11. Attractors of the stochastic system (3.1) with $k \in [0.0, 0.0006]$,and the initial point $(x_0, y_0, z_0) = (0.4, 0.3, 0.2)$ for: $(a)x_t$; $(b)y_t$; $(c)z_t$, with $l = 0.485$; $(d)x_t$; $(e)y_t$; $(f)z_t$, with $l = 0.495$;$(g)x_t$; $(h)y_t$; $(i)z_t$, with $l = 0.616$;$(j)x_t$; $(k)y_t$; $(l)z_t$, with $l = 0.640$; $(m)x_t$; $(n)y_t$; $(o)z_t$, with $l = 0.670$, where $a = 0.3, m = 5, k_1 = 0.3, \mu_2 = 0.2, \alpha_1 = 0.3, \alpha_2 = 4, \alpha_3 = 6$, and $k_2 = 0.2$

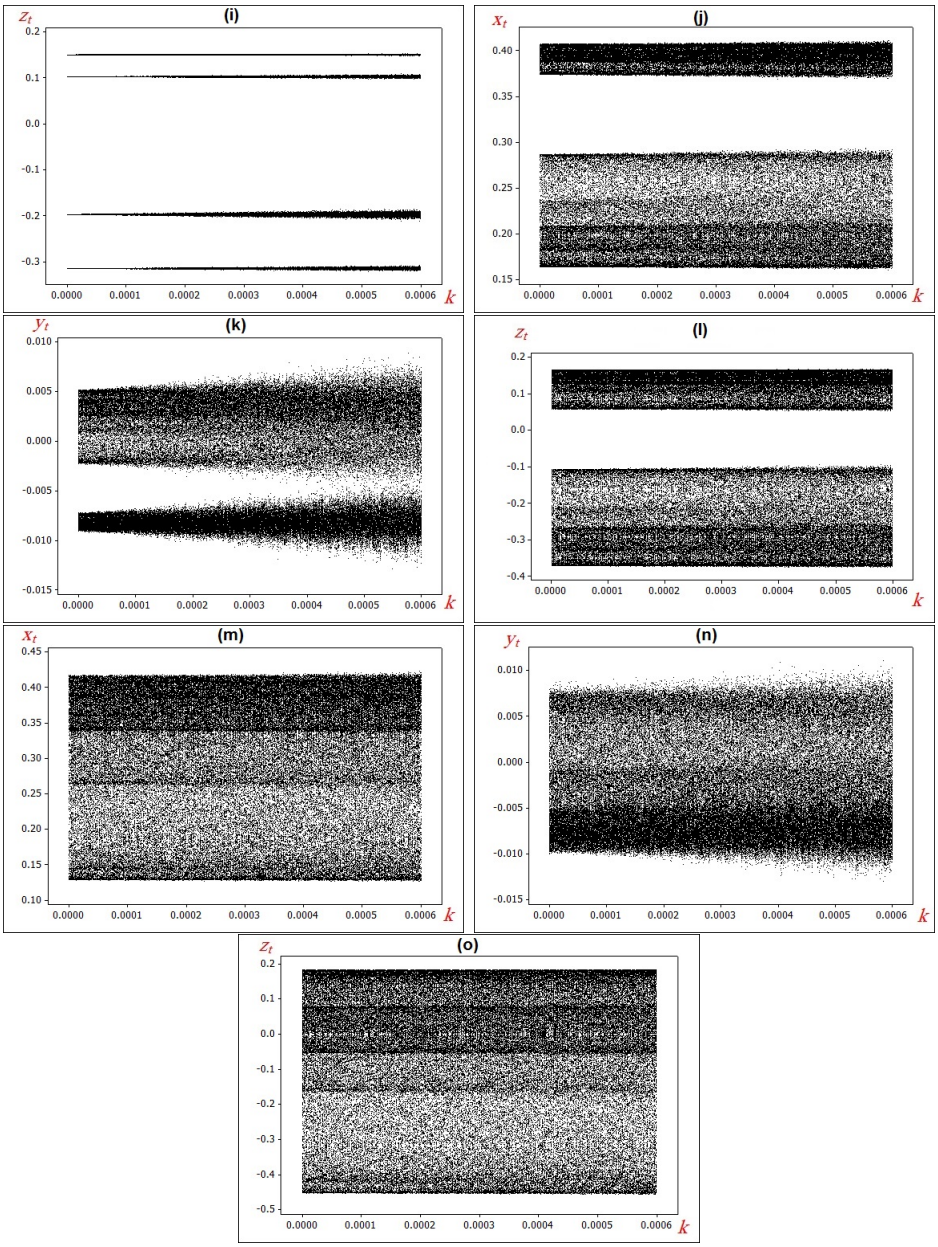

Figure 11. Continued

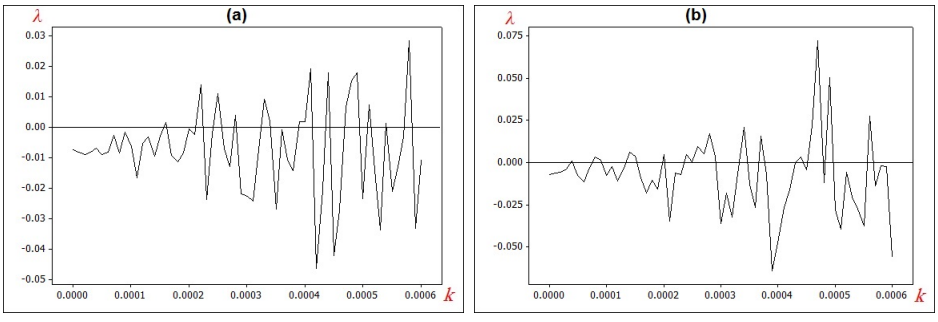

FIGURE 12. Lyapunov exponents of the stochastic system (2.2) with $k \in [0.0, 0.0006]$ and the initial point $(x_0, y_0, z_0) = (0.4, 0.3, 0.2)$ for: $(a) l = 0.490$; $(b) l = 0.4909$, where $a = 0.3, m = 5, k_1 = 0.3, \mu_2 = 0.2, \alpha_1 = 0.3, \alpha_2 = 4, \alpha_3 = 6$, and $k_2 = 0.2$.

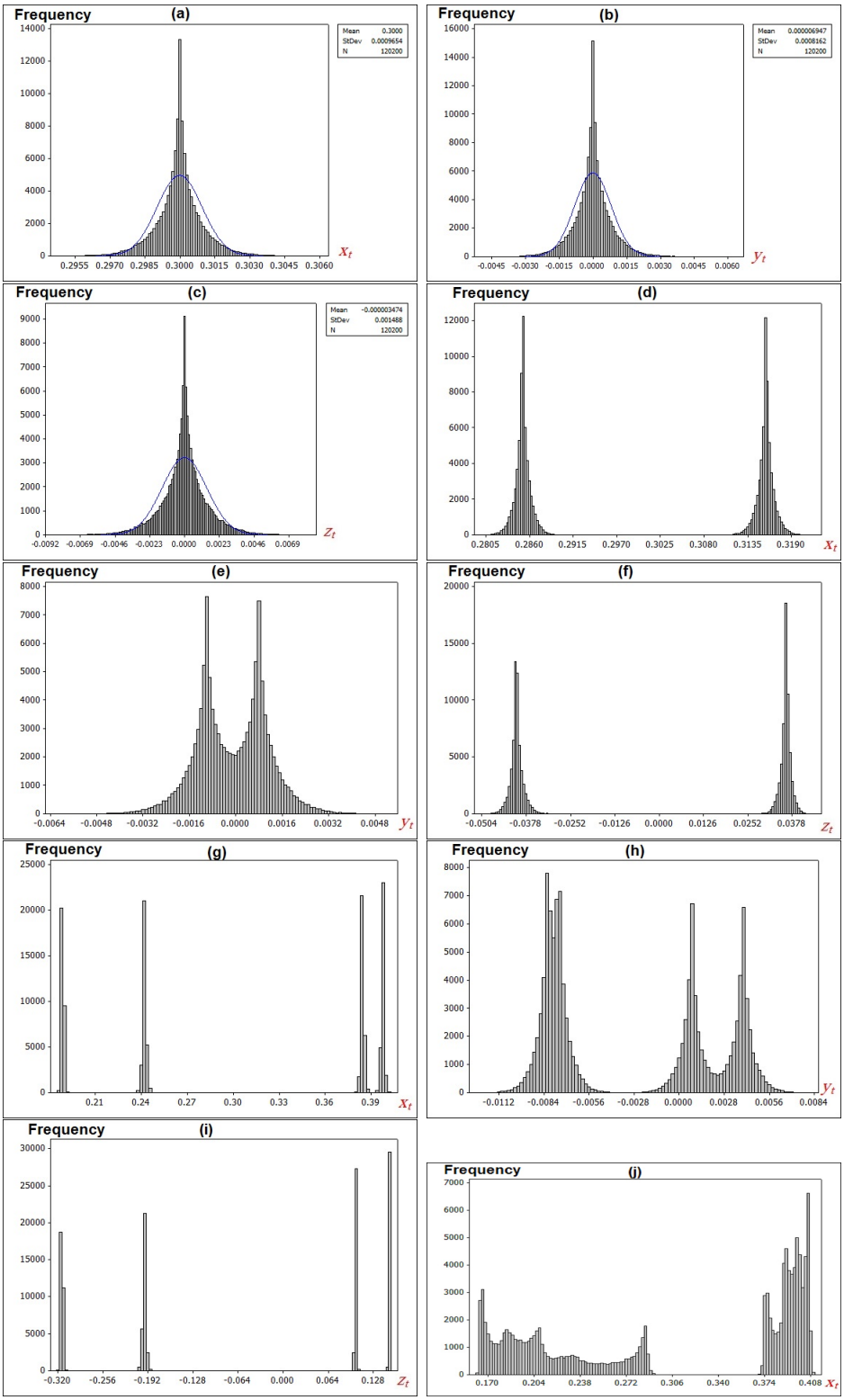

FIGURE 13. Asymptotic distributions of state variables (x_t, y_t, z_t) of the system (2.2) with $k \in [0.0, 0.0006]$,and the initial point $(x_0, y_0, z_0) = (0.4, 0.3, 0.2)$ for: $(a)x_t$; $(b)y_t$; $(c)z_t$, with $l = 0.485$; $(d)x_t$; $(e)y_t$; $(f)z_t$, with $l = 0.495$;$(g)x_t$; $(h)y_t$; $(i)z_t$, with $l = 0.616$;$(j)x_t$; $(k)y_t$; $(l)z_t$, with $l = 0.640$; $(m)x_t$; $(n)y_t$; $(o)z_t$, with $l = 0.670$, where $a = 0.3, m = 5, k_1 = 0.3, \mu_2 = 0.2, \alpha_1 = 0.3, \alpha_2 = 4, \alpha_3 = 6$, and $k_2 = 0.2$

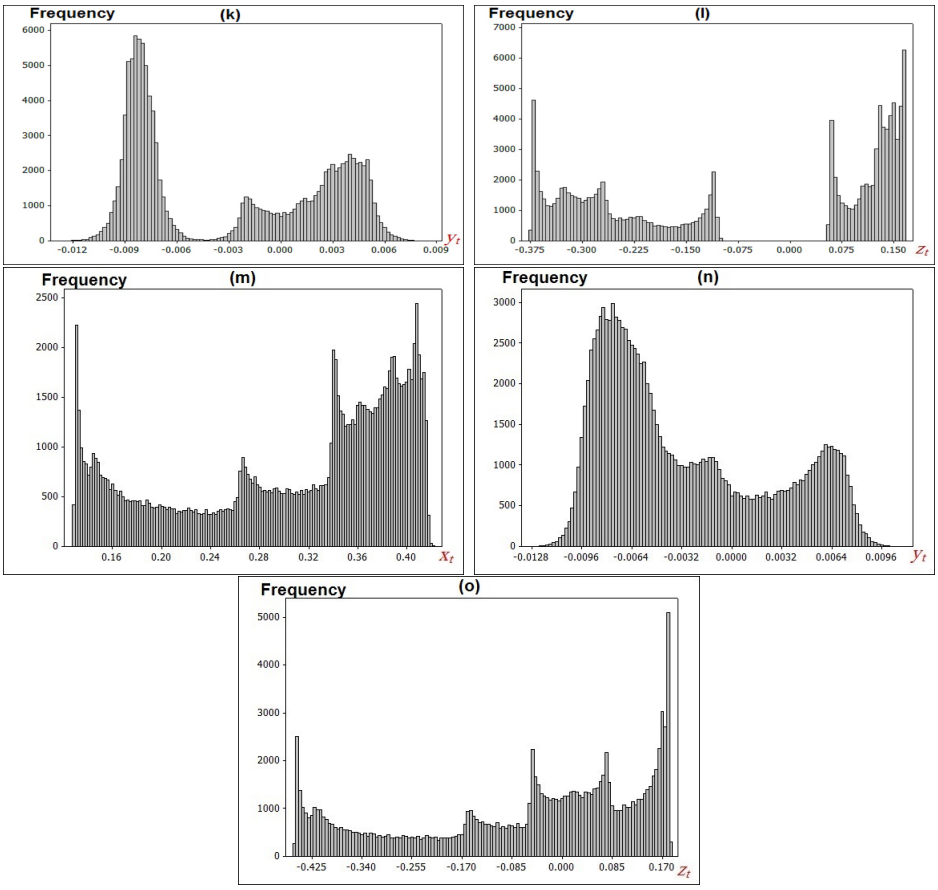

Figure 13. Continued